Nanoscale

ROYAL SOCIETY OF CHEMISTRY

MINIREVIEW

View Article Online
View Journal | View Issue

Cite this: *Nanoscale*, 2022, **14**, 1096

Enrichment of high-purity large-diameter semiconducting single-walled carbon nanotubes

Jingyi Wang and Ting Lei *

Semiconducting single-walled carbon nanotubes SWCNTs (s-SWCNTs) are considered one of the most promising alternatives to traditional silicon-based semiconductors. In particular, large-diameter s-SWCNTs (>1.2 nm) exhibit more advantages over small-diameter ones in high-performance electronic applications because of their higher charge carrier mobility and reduced Schottky barrier height. Great efforts have been made to enriching large-diameter s-SWCNTs from mass-produced raw CNTs that contain both metallic SWCNTs and s-SWCNTs. Among separation technologies, the effective and scalable ones are conjugated polymer wrapping (CPW), gel permeation chromatography (GC), aqueous two-phase extraction (ATPE), and density gradient ultracentrifugation (DGU). In this review, we survey recent progress on enriching large-diameter s-SWCNTs using those methods and outline the strategies and challenges in the separation according to the electronic type and chirality of SWCNTs. Finally, we highlight some applications of the enriched large-diameter s-SWCNTs and outlook for the future of SWCNT-based electronic devices.

Received 8th October 2021,
Accepted 5th December 2021

DOI: 10.1039/d1nr06635h

rsc.li/nanoscale

1. Introduction

Single-walled carbon nanotubes (SWCNTs) have drawn considerable attention in both academia and industry because of their unique electrical, optical, mechanical, and thermal properties. In particular, large-diameter (>1.2 nm) semiconducting SWCNTs (s-SWCNTs) have exhibited high charge carrier mobility, low Schottky barrier, and low-temperature processability. They are considered one of the most suitable materials to replace silicon for future high-performance electronics[1] and have been successfully used in high-performance digital circuits, flexible electronics, photovoltaics, thermoelectric devices, *etc.*[2–6]

Large-scale produced, commercially available SWCNTs are a mixture of s-SWCNTs and m-SWCNTs, as well as amorphous carbons and catalysts. Moreover, the as-produced SWCNTs, especially for large-diameter ones, bundle tightly together and have poor processability. Therefore, raw SWCNTs need to be dispersed and separated before use. To date, several enrichment methods, including conjugated polymer wrapping (CPW),[7] gel permeation chromatography (GC),[8] aqueous two-phase extraction (ATPE),[9] and density gradient ultracentrifugation (DGU)[10] have shown excellent capability in the enrichment of large-diameter s-SWCNTs. This review focuses on a

Key Laboratory of Polymer Chemistry and Physics (MOE), School of Materials Science and Engineering, Peking University, Beijing 100871, China.
E-mail: tinglei@pku.edu.cn

Jingyi Wang

Jingyi Wang received her B.S. degree in 2019 in Material Forming and Control Engineering from School of Materials Science & Engineering, Shandong University. She is currently pursuing her M.S. degree at Peking University. Her research interests mainly focus on carbon nanomaterials and their electrical applications, such as carbon-based field-effect transistors, logic circuits, etc.

Ting Lei

Ting Lei is an Assistant Professor in the Department of Materials Science & Engineering, Peking University. He received his B.S. and Ph.D. degrees from Peking University in 2008 and 2013. After postdoctoral training in Stanford University, he joined Peking University in 2018. His current research interests focus on organic/polymer functional materials, organic electronics, carbon-based electronics, and bioelectronics.

summary of recent progress on the state-of-the-art post-growth separation methods for enriching large-diameter s-SWCNTs and provides prospects for future enrichment development. Additionally, we discuss some important applications of the enriched large-diameter s-SWCNTs, and finally, give an outlook for future research and opportunities of large-diameter s-SWCNTs for next-generation optoelectronic devices.

2. Features of large-diameter s-SWCNTs

The structure of SWCNTs can be described by two chirality indices (n,m). Its diameter (d) and chiral angle (θ) can be calculated by equation (1) and (2):[11]

$$d = \frac{a}{\pi}\sqrt{n^2 + m^2 + nm} \quad (1)$$

$$\theta = \arctan\left(\frac{\sqrt{3}m}{2n+m}\right). \quad (2)$$

SWCNTs with the same chiral vectors can be further divided into left- and right-hand enantiomers. The diameters and chiralities of SWCNTs determine their electronic properties and potential applications. To date, s-SWCNTs extracted from several mass-production raw materials with different diameters have been explored for broad applications in various types of optoelectronics and biological imaging fields (Table 1).

To date, small-diameter SWCNTs (*e.g.*, CoMoCAT or HiPCO) have been widely used in photovoltaics, bioimaging, and photon emitters because they have suitable bandgaps and can be easily dispersed, purified, and functionalized.[12,15,19,20] For example, a recent simulation work proves that four small-diameter nanotube species, (6,4), (9,1), (7,3), and (7,5) with diameters of 0.69–0.76 nm, could form an idealized tandem solar cell having a sunlight harvesting potential of up to 28% while large-diameter nanotubes (1.01–1.47 nm) were predicted to have a sunlight harvesting efficiency of only 19%.[21] In addition, most well-defined single-chirality SWCNTs and enantiomers have been obtained in the small-diameter range.[22,23] However, small-diameter SWCNTs suffer from high production cost and poor electronic performance compared with their large-diameter counterparts.

Large-diameter s-SWCNTs (plasma-torch, arc-discharge and Tuball) tend to be longer, straighter, and have fewer defects, exhibiting higher charge carrier mobility.[24] s-SWCNTs with diameters larger than 1.2 nm have reduced Schottky barrier with the contact metal, which is helpful to increase carrier tunneling and decrease on-state resistance.[25] Therefore, large-diameter SWCNTs are important building blocks for electronic applications requiring high current density and high charge carrier mobility, such as high-performance computing (optimal d: ~1.5 nm[26]), thin-film transistors (TFTs), thermoelectrics, *etc.* Recently, Statz *et al.* demonstrated that s-SWCNTs with a diameter from 1.0 to 1.6 nm enable a large thermally accessible density of states (DoS), which leads to high Seebeck coefficients, low tunneling barriers and high conductivities for both electronic and thermoelectric applications.[18] Moreover, large-diameter SWCNTs can generate 1500–1600 nm fluorescence which is attractive for silicon-integrated optoelectronic devices for telecommunication technologies.[27] They have suitable endohedral volumes for guest molecule encapsulation. The newly created hybrid nanomaterials with modified properties are useful in photoconversion applications, such as photodetectors and photovoltaic devices.[19,28–30]

Nevertheless, large-diameter SWCNTs have stronger intertube interactions and tend to form strong and tight nanotube bundles, making them difficult to be individually dispersed and separated. The population of chiral candidates with similar diameters and electronic properties increases as the diameter increases, and therefore, the structural and property differences between the large-diameter SWCNTs decreases.[9] These challenges make the enrichment of large-diameter s-SWCNTs more difficult. Despite the challenges, many efforts have been devoted to enriching high-purity large-diameter s-SWCNTs and extracting large-diameter single-chiral carbon nanotubes because of their outstanding electronic performance and wide applications.

3. Enrichment methods

In recent years, both direct-controlled growth and post-growth separation methods have been developed for preparing SWCNTs with specific electronic types or chirality. Direct controlled growth can provide high purity s-SWCNTs or single-

Table 1 Properties and potential applications of s-SWCNTs extracted from several mass-production raw Materials[1]

	CoMoCAT	HiPCO	Plasma-torch	Arc-discharge	Tuball
Diameters (nm)	0.7–0.9	0.8–1.2	1.2–1.5	1.2–1.7	1.4–2.2
Band gaps (eV)	1.2–1.1	1.1–0.8	0.9–0.7	0.8–0.6	0.8–0.5
Costs (USD)	$300–700/g	$300–600/g	$10–40/g	$35–280/g	$4–20/g
TFT mobilities[a] (cm^2 $(V\ s)^{-1}$)	1–3	5–12	20–40	20–60	NA
Preferred optoelectronic applications	Photovoltaics and sensing[4,12–14]	Photonics and infrared photodetector[15,16]	TFTs and thermoelectrics[17,18]	TFTs and integrated circuits[2]	Not widely used in optoelectronics

[a] Data based on s-SWCNT random networks.

chirality SWCNTs. However, its high cost, poor tube quality, and low CNT density hinder its practical applications.[26,31] On the contrary, post-growth separation methods have advantages of simplicity, controllability, and high efficiency. Several of them allow high-purity (>99%) s-SWCNT separation and exhibit large-scale production capacity (Fig. 1). These methods are listed in Table 2. In general, these four methods are wet chemical techniques. They all need sonication/centrifugation processes to obtain well-dispersed SWCNTs with the presence of a dispersing agent, such as conjugated polymers, small molecular surfactants, and DNA, and use different types of solvents.

2.1. Conjugated polymer wrapping

Conjugated polymer wrapping is a powerful tool for enriching large-diameter s-SWCNTs and the highest purity has reached 99.9999%,[26] which was evaluated by electrical measurement. Polyfluorenes, polycarbozoles, polythiophenes, and their derivatives are commonly used as sorting polymers (Fig. 2a).[11] The sorting process mainly includes two steps: (1) dispersing SWCNTs with conjugated polymers by sonication and (2) separating s-SWCNTs and m-SWCNTs/impurities by centrifugation. It is believed that m-SWCNTs have more free electrons on surface, and they will exhibit stronger charge transfer with polymers. The charge transfer interactions make the m-SWCNT–polymer complex tend to form bundles in non-polar organic solvents and finally precipitate after ultracentrifugation.[37] Using conjugated polymers as the dispersant, SWCNT separation does not require extra medium, and the centrifuge force and period are found to be much lower than the surfactant-based processes.[38,39] However, it is based on organic solvents which are not environmentally friendly.

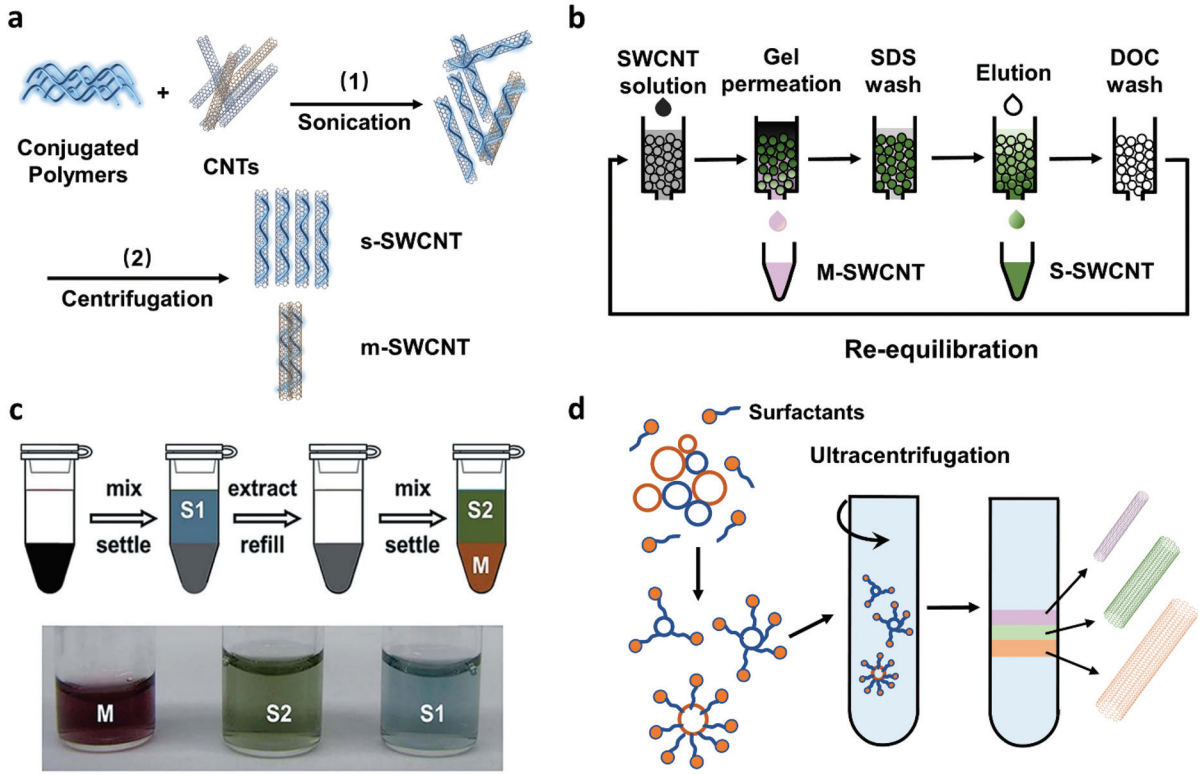

Fig. 1 Four solution-based post-growth separation methods. (a) Conjugated polymer wrapping (CPW). (b) Gel permeation chromatography (GC). (c) Aqueous two-phase extraction (ATPE). Reproduced with permission.[32] Copyright 2015, American Chemical Society. (d) Density gradient ultracentrifugation (DGU).

Table 2 Comparison of several large-diameter s-SWCNT enrichment methods

Method	Dispersant	Solvent	Separation medium	Highest purity reported	Capability for single-chirality enrichment	Yield	Cost	Mean length distribution[33]
CPW	Conjugated polymer	Organic solvent	NA	>99.9999%[26]	Low	High	Low	>1 μm
GC	Surfactant	Water	Sephacryl/Agarose	>99.9%[34]	High	Low	High	~0.6 μm
ATPE	Surfactant or DNA	Water	PEG/DX	>99.56%[35]	High	High	Low	NA
DGU	Surfactant	Water	Iodixanol	>99%[36]	Medium	Low	High	~0.6 μm

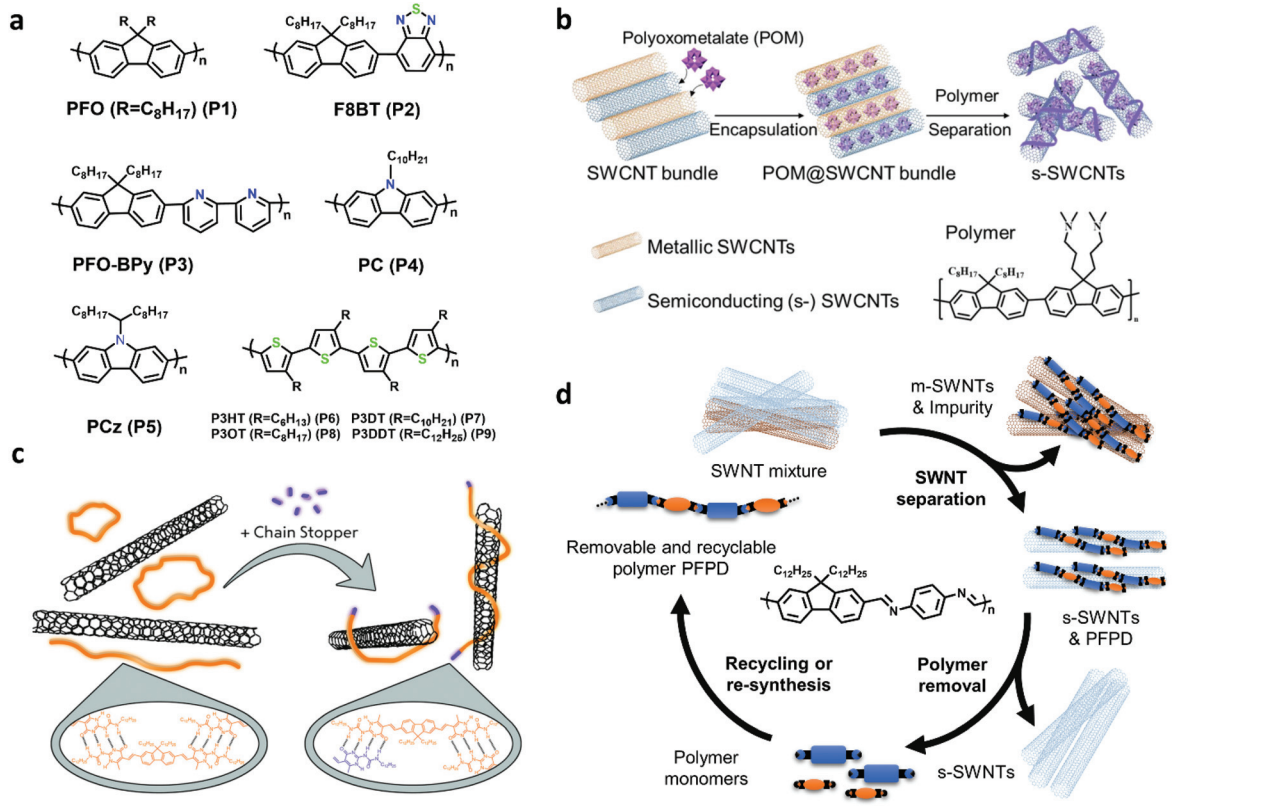

Fig. 2 (a) Conjugated polymers used for separate SWCNTs: Polyfluorenes(P1–P3), Polycarbazoles (P4, P5), Polythiophenes(P6–P9). (b) Schematic for SWCNTs encapsulated by redox polyoxometalates and s-SWCNTs separation using polymer wrapping. Reproduced with permission.[52] Copyright 2021, American Chemical Society. (c) Engineering supramolecular polymer conformation by introducing chain stoppers for efficient carbon nanotube sorting. Reproduced with permission.[53] Copyright 2020, John Wiley and Sons. (d) Diagram of s-SWCNTs separation circle of removable and recyclable polymer PFPD.

The structure of conjugated polymer plays an important role in enriching different diameter s-SWCNTs. For example, poly(9,9-di-*n*-octylfluorenyl-2,7-diyl) (PFO, P1) and poly(*N*-decyl-2,7-carbazole) (PC, P4) are not favorable for extracting s-SWCNTs with diameters larger than 1.1 nm.[40,41] By adding rigid and planar conjugated building blocks, like benzothiadiazole(P2) and pyridine(P3), to the backbone, polymers can enrich large-diameter s-SWCNTs produced by arc-discharge, and the purity is higher than 99.9%.[42–46] Several groups found that polymers with longer alkyl chains (P5, P9) could enrich larger-diameter s-SWCNTs.[37,47,48] In addition, parameters, such as the molecular weight, polymer concentration, polymer to SWCNTs ratio, and temperature, will also affect the diameter selectivity. Enrichment of s-SWCNTs with different diameters with the same polymer has been achieved by altering those parameters.[40,49–51]

The diameter and purity of s-SWCNTs sorted by conjugated polymer wrapping have satisfied the requirement of a wide range of electronic applications. The devices made from the polymer-wrapped s-SWCNTs show excellent performance. The biggest challenge for this method may be its deficiencies in extracting specific nanotube species, especially in the large-diameter range. Several groups reported that enhanced interaction between polymers and specific (*n*,*m*) SWCNTs could promote chiral selectivity and reduce diameter distribution. For example, it is reported that P8BT (P2) could enrich (15,4) s-SWCNTs (d = 1.36 nm).[42,44] Tange *et al.*[44] attributed the selectivity to the structure and energy matching between P8BT and (15,4) SWCNT. Several other reports also demonstrated that it is promising for single-chirality s-SWCNT enrichment if polymers could wrap SWCNTs with a preferred stacking path or a good alignment.[54,55] Recently, Li *et al.* used polymers with the diameter or chiral angle selectivity to successfully enrich (10,8) (d = 1.24 nm) and (12,5) (d = 1.2 nm) s-SWCNTs with a high single-chirality purity larger than 90%, and the optical and electrical performances of the purified s-SWCNTs were still excellent.[56] They developed two novel methods, namely, enhanced ultracentrifugation (ultracentrifugation under a suitable centrifugal force and time) and stepwise extraction processing (an alternating process of CPW purification with different polymers), which paves a way for future chirality enrichment of large-diameter SWCNTs. Moreover, endohedral filling effects were used for modulating the interaction between polymers and SWCNTs. Yang *et al.* filled redox polyoxometalates in SWCNTs and successfully enriched s-SWCNTs with a narrow diameter distribution (centered at 1.3–1.4 nm)

(Fig. 2b).[52] They attributed the enrichment to different degrees of oxidation between redox clusters and nanotubes with different metallicity and diameters, which finally modifies the binding affinity between polymers and the SWCNTs.

In addition, polymer contamination is a severe problem in the CPW method. Excess polymers need to be removed because they will significantly affect the charge transport property and reduce device stability. Therefore, removable and recyclable polymers have been developed, such as supramolecular polymers (SMP), imine-bonded conjugated polymers, and foldable polymers.[1] Supramolecular polymers (SMP) and imine-bonded polymers have exhibited high separation ability for large-diameter s-SWCNTs. Recently, Gao *et al.* reported a conformation control method to improve the sorting yield of supramolecular polymer, and they improved the sorting yield by twice (from 7% to 14%) without losing purity (>99%) (Fig. 2c).[53] Lei *et al.* synthesized imine-based polymer PFPD for sorting plasma-torch SWCNTs and achieved both high purity (99.7%) and high yield (23.7%) (Fig. 2d).[57] Recently, they further improved the semiconducting purity to 99.997% after an additional purification step.[3] When using removable and recyclable polymers, the decomposed monomers can be recycled for polymer resynthesis and reuse, which helps lower the sorting costs.

2.2. Gel permeation chromatography (GC)

Using GC, SWCNTs can be effectively separated by metallicity, diameter, and chirality. Sodium dodecyl sulfate (SDS), sodium cholate (SC), and sodium deoxycholate (DOC) are commonly used dispersants and eluents (Fig. 3a). These surfactants can form different coating sizes, shapes, or thicknesses around different types of SWCNTs according to their surface π-electron states,[58] modulating the interactions of SWCNTs with the gel and therefore influencing SWCNT separation. SDS has been studied more thoroughly compared with other surfactants. It is believed that SDS has electrical and bandgap selectivity. It tends to form packed and dense micelles on the surface of m-SWCNTs, which weakens the SWCNT/gel interaction and promotes m-SWCNT elution. After m-SWCNTs, the larger diameter s-SWCNTs first elute, and then the smaller diameter ones[59] (Fig. 3b).

GC has been successfully used in sorting small-diameter s-SWCNT species (*e.g.*, CoMoCAT and HiPCO SWCNTs) in a mass-production manner and obtained a single-chirality purity up to 98%.[60–62] Nevertheless, separation of large-diameter s-SWCNTs still faces the problems of higher surfactant package densities and lower absorbability to the gel, as well as a reduced (*n*,*m*) resolution because of decreased structure differences.[8] Temperature and pH are critical factors for controlling the absorbance and coverage of surfactants.[58,60,62–64] Usually, improving the GC temperature will desorb the wrapped surfactants or make them loosely packed, thus increasing the interaction between SWCNTs and the gel. pH could change the number of wrapped surfactants by affecting the oxidation of SWCNTs or altering the surfactant micelle structure.[58] Wang *et al.* reported a record semiconducting purity above 99.94% by tuning the pH value of the surfactant solution.[64] Yang *et al.* achieved a structural separation of s-SWCNTs with diameters ranging from 1.2 to 1.7 nm by a NaOH-assisted gel chromatography method.[8] They proposed that the introduction of NaOH could reduce the oxidation of SWCNTs and decrease the SDS coverage, therefore enhancing the interaction of large-diameter SWCNTs with gel and assisting separation of SWCNTs with different structures. Using mixed surfactants with a proper concentration could help to amplify the interaction difference between various SWCNTs with gel, which is also beneficial for separating large-diameter s-SWCNTs. Several groups have reported successful enrichments of high-purity large-diameter s-SWCNTs using a mixture of SDS and SC.[8,65] Studies found that SC absorbs and binds tighter than SDS on the SWCNTs, reducing SDS absorbance and increasing the interaction difference of large-dia-

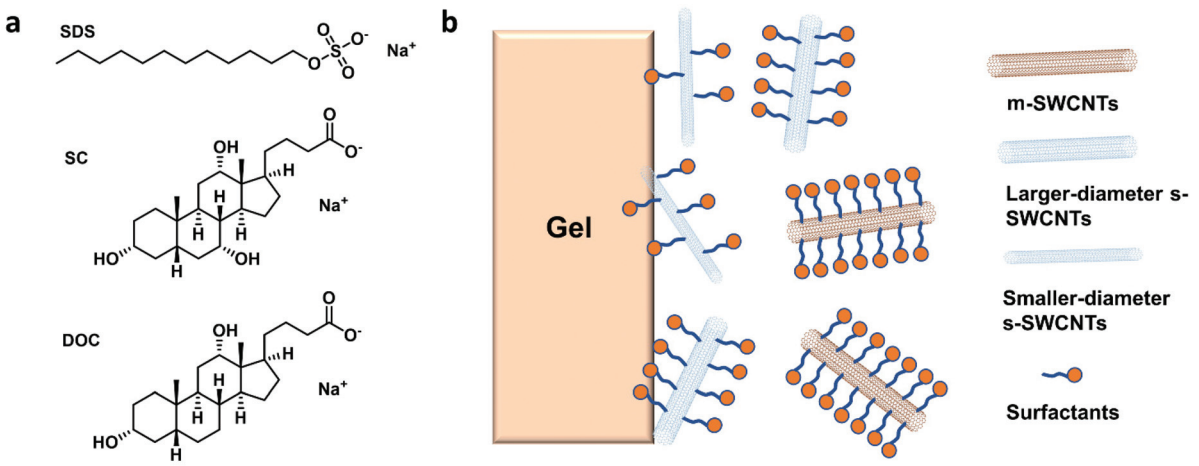

Fig. 3 (a) Chemical structure of three commonly used surfactants. (b) Schematic diagram of SDS wrapping and sorting mechanism. The number and density of SDS on SWCNT surface: m-SWCNTs > large-diameter s-SWCNTs > small-diameter s-SWCNTs. The interaction strength with the gel: small-diameter s-SWCNTs > large-diameter s-SWCNTs > m-SWCNTs.

meter species with the gel.[65] Using mixed SDS and SC, Wang *et al.* successfully separated mixed s-SWCNTs species with mean diameters of 1.30, 1.38, 1.45, and 1.58 nm.[66] Later, they found that DOC displays good selectivity for different diameters. They achieved high-purity single-chirality separation using triple surfactants as the eluent. However, adding DOC as an ingredient in the eluent can only efficiently separate pure-chirality s-SWCNTs under 1 nm (Fig. 4).[59,62] Therefore, a more suitable surfactant mixture, surfactant concentration, and optimized external conditions need to be explored for larger-diameter SWCNT separation.

The gel medium also plays an important role in SWCNT separation. Clar and Zanoni *et al.* studied a series of commercially available hydrogels for the GC separation method.[67,68] Their results show that the chemical composition, pore size, and charge moieties of hydrogels are closely related to specific absorbance sites for SWCNTs, which can be tuned for improving selectivity and yield. Moreover, the commonly used gel medium (Sephacryl S-200) is expensive, limiting the practical usage of the GC method for scalable enrichment of s-SWCNTs. To address the cost issue, several groups began to develop low-cost gels for SWCNT separation.[69–72] Khamidullin *et al.* used nitrated cotton wool as the gel medium and successfully extracted s-SWCNTs from Tuball tubes.[71] However, the reported purity of s-SWCNTs using these low-cost gels is no more than 98.7%.[72]

2.3. Aqueous two-phase extraction (ATPE)

ATPE uses two immiscible phases, polyethylene glycol (PEG) and dextran (DX), to separate surfactant/DNA-coated SWCNTs with different metallicity and chirality.[73,74] SWCNTs can be separated into more hydrophobic, upper PEG-rich phase or less hydrophobic, lower DX-rich phase depending on their different solvation energy and equilibrium affinity for those two phases. Because DNA is mostly used for sorting small-diameter species, we will not discuss DNA-based ATPE in this review. ATPE is able to separate both pure-chirality semiconducting and metallic SWCNTs, unlike GC or polymer wrapping, which is effective only for separating semiconducting species.

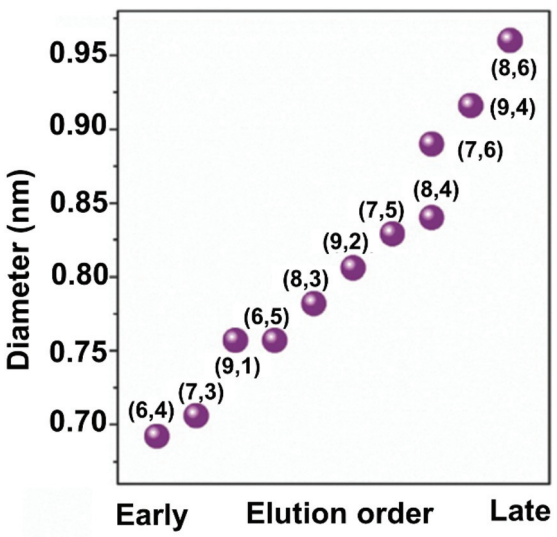

Fig. 4 Diameter separation of single-chirality use triple surfactants (0.5 wt% SDS + 0.5 wt% SC + *y* wt% DOC, *y* is increased from 0.019 to 0.085 with an incremental step of 0.002 wt% to 0.003 wt%.) as the eluent. Elution order is constant with DOC concentration. Reproduced with permission.[59] Copyright 2017, John Wiley and Sons.

For large-diameter SWCNTs (>1.2 nm), the metallic/semiconducting tube separation automatically happened using the PEG-DX-SDS/SC system.[73] It was proposed that m-SWCNTs' large polarizability renders them more hydrophilic than s-SWCNTs, and tend to be enriched in the bottom DX phase. Wei *et al.* explored the upper limit purity of s-SWCNTs of ATPE separation using the above commonly used system. They found that the s-SWCNT purity was more than 99.5% after 6–8 cycles of iterative sorting.[35] Adjusting the redox condition of the ATPE system can modulate m-SWCNT/s-SWCNT separation because different oxidation state of SWCNTs can induce different degree of electron transfer and surfactant reorganization on the SWCNT surface[32] (Fig. 5a). In addition, adding a small amount of oxidizing agent, such as ~mM NaClO, could help make the redox potential of ATPE system more fixed than without any oxidant, making the separation more reliable and robust.

Using the PEG-DEX-SDS/DOC or PEG-DEX-SDS/SC/DOC system can realize single-chirality enrichment.[9,75,76] The separation mechanism is probably related to the competition between surfactants, for which one will primarily adsorb on the surface of specific chirality SWCNTs.[9] Generally, the affinity order is DOC > SC > SDS. SWCNTs mainly coated with DOC or SC tend to stay in the DX phase while SWCNTs coated with SDS prefer to stay in the PEG phase. Therefore, a suitable concentration of surfactants is vital to refine the chirality distribution of SWCNTs, as well as decrease the number of enrichment steps. Fagan *et al.* established an empirical formula about the SDS content and the SWCNT diameter or species at a fixed DOC content: d = 0.284 nm SDS^{-1} (%) + 0.48.[75] They demonstrated that 1.6–1.8 nm diameter SWCNTs could be discriminated at ~0.1% DOC and 0.7–0.15% SDS. Combining mixed surfactants with pH adjustment is demonstrated to enhance the separation of large-diameter SWCNTs species. Recently, Li *et al.* successfully separated specific large-diameter single-enantiomer SWCNTs (1.41 nm, (14,6)) by adding HCl to assist ATPE separation.[9] Adding acid to the system can alter the structure of DOC and SC, make them detach from SWCNTs and increase SDS absorption, finally, push species coated with the most SDS to PEG phase (Fig. 5b). By controlling pH, one can carry out the enrichment of SWCNTs with reduced iterations or without changing the global surfactant concentrations.[74]

2.4. Density gradient ultracentrifugation (DGU)

The main process of DGU includes three steps: (1) dispersing SWCNTs with ultrasonication and ultracentrifugation to remove impurities like metallic catalysts and amorphous

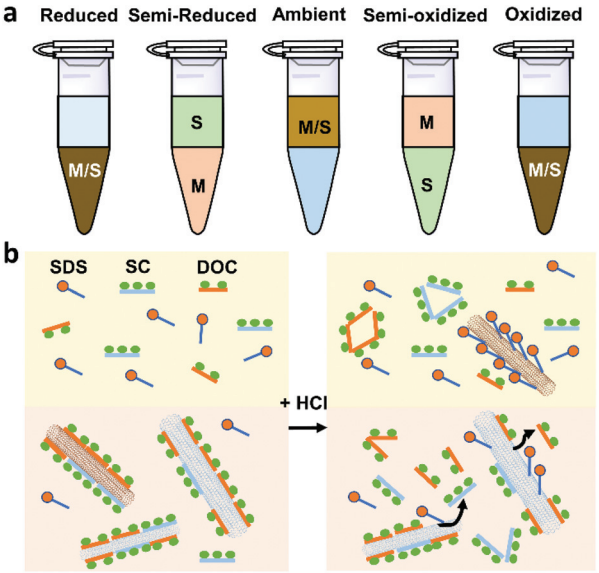

Fig. 5 (a) AD SWCNTs partition in a redox modulated PEG/DX ATPE system. From left to right is: a "reduced" regime, both m-SWCNTs and s-SWCNTs stay in DX phase; a "semi-reduced" regime, m-SWCNTs and s-SWCNTs stay in PEG and DX phase, respectively; (3) an "ambient" regime, both m-SWCNTs and s-SWCNTs stay in PEG phase; a "semi-oxidized" regime, m-SWCNTs and s-SWCNTs stay in DX and PEG phase, respectively; an "oxidized" regime, both m-SWCNTs and s-SWCNTs bake to DX phase again. (b) Diagram of the pH-driven SWCNT separation. Before adding HCl, nanotubes are wrapped mostly by DOC and SC, and all SWCNTs stay in the less hydrophobic DX phase. After adding HCl, DOC and SC are aggregated due to the protonation of the carboxylic acid and taken off from the surface of SWCNTs. Therefore, more SDS begins to coat around SWCNTs and drive nanotubes migrate to the top PEG phase.

carbon; (2) forming an initial linear or nonlinear density gradient by mixing iodixanol, surfactants, and water with an appropriate density; and (3) adding SWCNT dispersion into the medium and performing long-term, high-speed ultracentrifugation to separate SWCNTs with different densities. After the procedures, SWCNTs with different metallicity, diameter, and chirality can be separated into different layers in the density gradient medium. This method is also effective for separating empty and filled SWCNTs.[77] It can enrich both high purity (>99%) s-SWCNTs and m-SWCNTs with large diameters.[36,78]

The strategy used for m-SWCNT/s-SWCNT separation is based on regulating the surfactant proportions. Many studies demonstrated that a 3 : 2 or 4 : 1 ratio of SDS/SC could enrich high-purity m-SWCNTs while a 1 : 4 ratio of SDS/SC can enrich high-purity s-SWCNTs when their concentrations are around 1% w/v.[39,78,79] For realizing tight diameter distributions of s-SWCNTs, Seo *et al.* reported a dual-iteration DGU method: initially using SC to purify raw materials and extract well-coated SWCNT species followed by using the SDS/SC co-surfactant to isolate s-SWCNTs.[36] Using this method, they could enrich ~1.6 nm s-SWCNTs consisting of several chiralities, including the (18,4), (19,2), and (20,0) tubes. Furthermore, they enriched ~1.4 nm s-SWCNTs by adding NaCl to the dispersion because excess sodium ions could lead to preferential aggregation of larger-diameter species.

DGU methods with a nonlinear density profile media have been developed to improve the resolution for diameter separation. Nonlinear DGU was able to separate SWCNTs with different chiralities and several pairs of enantiomers. However, the largest separated single-chiral tube is (8,6) with a diameter around 1 nm.[80] Although this technology is readily scalable for industrial production, its ability for extracting pure-chirality large-diameter s-SWCNTs needs to be further explored. Moreover, this technology faces several severe issues, such as time-consuming, high-cost, low-yield, and difficulties in preparing density gradient media. Therefore, more studies focus on the other three methods, and DGU has not been greatly developed in recent years.

4. Applications of large-diameter s-SWCNTs

Compared with small-diameter ones, large-diameter s-SWCNTs have many advantages, such as higher charge carrier mobility, smaller contact resistance, and larger current density. These features are especially desired for carbon-based integrated circuits,[25] like high-speed ring oscillators (ROs),[81,82] radio-frequency (RF) transistors,[83,84] as well as thin-film transistors (TFTs) for flexible electronics.[3,85] Tulevski *et al.* pointed out that based on the modeling results, using small-diameter (<1 nm) s-SWCNTs, the threshold voltage (V_t) variation of a transistor could greater than 1 : 1 ratio impact on V_t, while using large diameters (>1.4 nm) leads to much less impact on V_t.[25] However, larger diameters (*e.g.*, >1.8 nm) could lead to a high off current due to a smaller bandgap.

Except for purity requirements, well-defined and high-density aligned s-SWCNT films are critical for reducing inter-tube resistance and providing sufficient driving ability.[25] Various SWCNT alignment methods have been reported, and several reviews discussed them in detail.[20,86,87] Recently, Liu *et al.* made significant progress: they achieved 99.9999% purity s-SWCNTs arrays with a packing density of adjustable 100–200 tubes per micrometer using a dimension-limited self-alignment (DLSA) procedure (Fig. 6a).[26] More recently, the same group fabricated 11-stage ring oscillators (ROs) with a record propagation gate delay of 11.3 ps exceeding all ROs made by other nanomaterials.[83] However, this method faces the problems of SWCNT bundling and limited uniformity. Gao *et al.* invented a method to suppress bundle formation by introducing inter-tube electrostatic repulsion, providing a possible approach for reducing bundles and increasing uniformity over a large area(Fig. 6b).[88]

Despite the advantages of aligned nanotube films, random SWCNT networks show a higher uniformity in a large area and a higher device yield, ready for high-volume semiconductor manufacture. For example, Bishop *et al.* developed a method for uniformly depositing SWCNTs over a large-area industry-standard substrate (at least 200 mm-diameter wafer) which

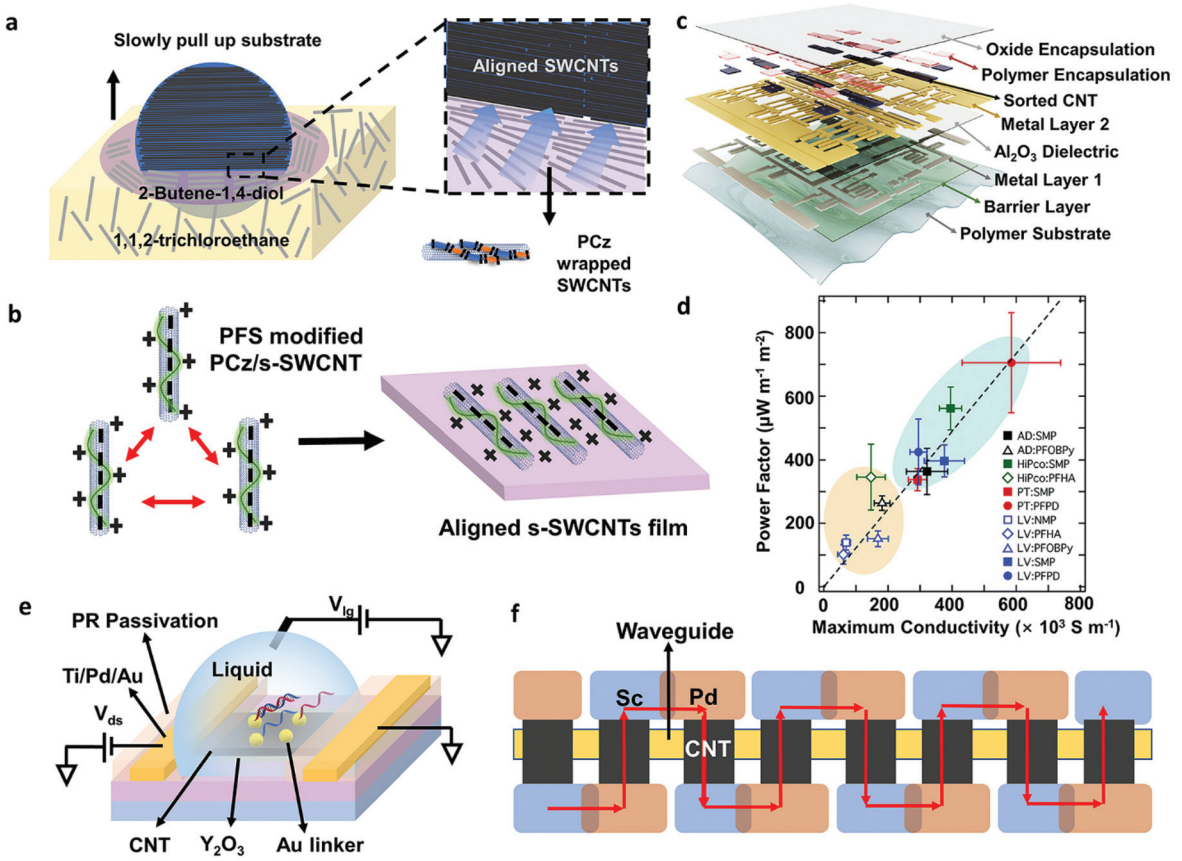

Fig. 6 (a) Schematic images of DLSA procedure to assemble aligned-SWCNT arrays on a 4-inch wafer. The purple layer is formed by 2-butene-1,4-diol ($C_4H_8O_2$). As the wafer is slowly pulled out, the possible hydrogen bonds between polymers and $C_4H_8O_2$ allowed the confined on the interface between two insoluble solvents and assembled onto the wafer surface along the contact line. (b) Schematic illustration of a positively charged conjugated molecule, proflavine hemisulfate (PFS), modifying the surface of PCz wrapped s-SWCNTs. The positive charges can prevent the aggregation of s-SWCNTs during alignment. (c) Layer structure of the digital and analog circuits build on a flexible substrate. Reproduced with permission.[3] Copyright 2019, Springer Nature. (d) Relationship between maximum thermoelectric (TE) power factor (optimally doped network) and the maximum conductivity (fully doped network) for different types of sorted s-SWCNT networks. The maximum conductivity and TE power factor for s-SWCNT networks using removable polymers (SMP, PFPD, blue oval) are larger than the values for s-SWCNT networks sorted with non-removable polymers (PFOBPy, PFHA, orange oval). Among them, plasma-torch s-SWCNT network with PFPD exhibited the highest TE power factor. Reproduced with permission.[89] Copyright 2017, Royal Society of Chemistry. (e) Schematic diagram of a carbon nanotube floating-gate FET biosensor. The ultrathin high-k Y_2O_3 passivation layer is helpful to amplify response and improve sensitivity. (f) Schematic diagram of a series carbon nanotube photodetector device contains eight cells. Red arrows represent a current direction at forward bias. The cells are connected by a pair of overlapping Sc and Pd electrodes.

allows carbon nanotube transistors to be fabricated in a commercial silicon manufacturing facility.[90] Additionally, the random SWCNT network is easy to deposit, exhibits reliability, flexibility, and little device variation, making it suitable for large-area flexible electronics. Hills *et al.* successfully demonstrated a 16-bit modern microprocessor containing more than 14 000 complementary metal–oxide-semiconductor (CMOS) carbon nanotube FETs by carefully designing electronic circuits and manufacturing procedures to overcome material defects and transistor variations.[2] Lei *et al.* fabricated flexible digital and analog circuits based on nanotube networks by simple soaking method. They achieved a >99.9% transistor yield and a state-of-the-art performance on a flexible substrate (Fig. 6c).

Except for TFT arrays and circuits, some thermoelectric, sensing, and photoelectric devices are also developed profiting from the unique properties of large-diameter SWCNTs.[91–94] Macleod *et al.* fabricated both *p*- and *n*-type thermoelectric generators based on plasma-torch s-SWCNTs enriched by removable polymers PFPD (Fig. 6d). They achieved a thermoelectric power factor of over 700μW m^{-1} K^{-2} at 298 K, which is among the highest metrics for SWCNT and polymer thermoelectric materials.[89] Although theoretical prediction shows that small-diameter s-SWCNTs have theoretically larger maximum thermopower (Seebeck coefficient, *S*), the high mobility and high doped electrical conductivity of large-diameter s-SWCNTs make them exhibit better thermoelectric properties (power factor, *PF*) when forming carbon nanotube networks. Additionally, the results revealed that aligned carbon nanotubes with reduced tube–tube junctions are also important to improving the electrical conductivity and TE performance of

solution-processed s-SWCNT networks. Liang *et al.* reported wafer-scale, label-free, and highly stable carbon nanotube biosensors for biomarker detection (Fig. 6e). They used a floating-gate structure with a high-k ultrathin Y_2O_3 layer to amplify response and improve sensitivity. They successfully detected DNA sequences and microvesicles down to 60 aM and 6 particles per mL, respectively.[95] Ma *et al.* used arc-discharge s-SWCNTs as the active material for photodetectors and logic circuits and developed an optoelectronic integrated system (Fig. 6f).[92] The photodetectors based on carbon nanotubes exhibit 12.5 mA W^{-1} photoresponsivity at 1530 nm with the silicon-waveguide. Their work demonstrated large-diameter s-SWCNTs as a potential material for future electrically driven on-chip sensing and fiber-optic telecommunication.

Despite the successful implementation of s-SWCNTs in a wide range of electronic applications, further developments are still required. First, SWCNTs with higher purity and narrower diameter distribution are needed to decrease device variations in large-scale integrated circuits. Second, pure-chirality SWCNTs are more desired in photoelectric emission and absorption devices for their well-defined emission wavelengths and narrow absorbance peaks. Endohedral encapsulation provides an idea for further enhancing optical properties. Third, post-growth enrichment methods introduce a large number of surfactants or polymers onto SWCNTs which negatively affects the properties of the nanotubes. Therefore, minimum introduction and complete removal of those dispersants need more studies and exploration. The settlement for these problems is closely related to the development of controllable technologies for pure single metallicity or chirality SWCNT enrichment.

5. Conclusions and outlook

In this review, we introduced four mainstream, potentially scalable separation methods for enriching large-diameter s-SWCNTs. Among these methods, CPW produces the highest semiconducting purity while the single-chirality enrichment is insufficient, and it has severe polymer contamination issues. GC could enrich high purity and high yield single-chirality species but is only effective for small-diameter semiconducting carbon nanotubes. Although ATPE is the latest reported method, it is possible to extract large-diameter SWCNT species regardless of their metallicity. However, the purity of s-SWCNTs is lower than the above methods. DGU is a powerful technique in separating large-diameter SWCNTs with a narrow diameter distribution, but this technique needs long-term, high-speed ultracentrifugation with a low yield. Therefore, using a single purification method seems challenging to obtain both high semiconducting purity and single-chirality purity in a low-cost manner. We believe that combining different enrichment methods and integrating their advantages for purification may be a feasible approach. For example, after the ATPE separation based on surfactants, exchanging the surfactants with DNA can generate pure-chirality SWCNT samples.[96,97] In addition, the sorting mechanism of these methods is not fully understood, and more theoretical and experimental studies are required. Simplifying the enrichment protocols, increasing the purity and yield of SWCNTs with specific metallicity, diameter, chirality, and enantiomers are still desirable for practical applications of sorted SWCNTs in various optoelectronic fields.

Author contributions

Writing—original draft, J. W.; writing—review and editing, T. L. All the authors have read and agreed to the published version of the manuscript.

Conflicts of interest

There are no conflicts to declare.

Acknowledgements

This work is supported by the Beijing Municipal Natural Science Foundation (2192020) and the Key-Area Research and Development Program of Guangdong Province (2019B010934001).

References

1 T. Lei, I. Pochorovski and Z. Bao, *Acc. Chem. Res.*, 2017, **50**, 1096–1104.
2 G. Hills, C. Lau, A. Wright, S. Fuller, M. D. Bishop, T. Srimani, P. Kanhaiya, R. Ho, A. Amer, Y. Stein, D. Murphy, Arvind, A. Chandrakasan and M. M. Shulaker, *Nature*, 2019, **572**, 595–602.
3 T. Lei, L.-L. Shao, Y.-Q. Zheng, G. Pitner, G. Fang, C. Zhu, S. Li, R. Beausoleil, H. S. P. Wong, T.-C. Huang, K.-T. Cheng and Z. Bao, *Nat. Commun.*, 2019, **10**, 2161.
4 L. Wieland, H. Li, C. Rust, J. H. Chen and B. S. Flavel, *Adv. Energy Mater.*, 2021, **11**, 2002880.
5 J. L. Blackburn, A. J. Ferguson, C. Cho and J. C. Grunlan, *Adv. Mater.*, 2018, **30**, 1704386.
6 L. Sacco, S. Forel, I. Florea and C. S. Cojocaru, *Carbon*, 2020, **157**, 631–639.
7 L. Xu, M. Valasek, F. Hennrich, R. Fischer, M. M. Kappes and M. Mayor, *Macromolecules*, 2021, **54**, 4363–4374.
8 D. H. Yang, J. W. Hu, H. P. Liu, S. L. Li, W. Su, Q. Li, N. G. Zhou, Y. C. Wang, W. Y. Zhou, S. S. Xie and H. Kataura, *Adv. Funct. Mater.*, 2017, **27**, 1700278.
9 H. Li, G. Gordeev, O. Garrity, N. A. Peyyety, P. B. Selvasundaram, S. Dehm, R. Krupke, S. Cambre, W. Wenseleers, S. Reich, M. Zheng, J. A. Fagan and B. S. Flavel, *ACS Nano*, 2020, **14**, 948–963.
10 M. Kawai, H. Kyakuno, T. Suzuki, T. Igarashi, H. Suzuki, T. Okazaki, H. Kataura, Y. Maniwa and K. Yanagi, *J. Am. Chem. Soc.*, 2012, **134**, 9545–9548.

11 J. Y. Wang and T. Lei, *Polymers*, 2020, **12**, 1548.
12 L. Wieland, C. Rust, H. Li, M. Jakoby, I. Howard, F. Li, J. Shi, J. Chen and B. S. Flavel, *Carbon*, 2021, **184**, 828–835.
13 V. Zubkovs, S. J. Wu, S. Y. Rahnamaee, N. Schuergers and A. A. Boghossian, *Chem. Mater.*, 2020, **32**, 8798–8807.
14 X. Z. Xu, P. Clement, J. Eklof-Osterberg, N. Kelley-Loughnane, K. Moth-Poulsen, J. L. Chavez and M. Palma, *Nano Lett.*, 2018, **18**, 4130–4135.
15 M. Balestrieri, A. S. Keita, E. Duran-Valdeiglesias, C. Alonso-Ramos, W. W. Zhang, X. Le Roux, E. Cassan, L. Vivien, V. Bezugly, A. Fediai, V. Derycke and A. Filoramo, *Adv. Funct. Mater.*, 2017, **27**, 1702341.
16 L. Chio, R. L. Pinals, A. Murali, N. S. Goh and M. P. Landry, *Adv. Funct. Mater.*, 2020, **30**, 1910556.
17 L. Nela, J. S. Tang, Q. Cao, G. Tulevski and S. J. Han, *Nano Lett.*, 2018, **18**, 2054–2059.
18 M. Statz, S. Schneider, F. J. Berger, L. L. Lai, W. A. Wood, M. Abdi-Jalebi, S. Leingang, H. J. Himmel, J. Zaumseil and H. Sirringhaus, *ACS Nano*, 2020, **14**, 15552–15565.
19 J. Campo, S. Cambre, B. Botka, J. Obrzut, W. Wenseleers and J. A. Fagan, *ACS Nano*, 2021, **15**, 2301–2317.
20 M. S. He, S. C. Zhang and J. Zhang, *Chem. Rev.*, 2020, **120**, 12592–12684.
21 M. Pfohl, K. Glaser, A. Graf, A. Mertens, D. D. Tune, T. Puerckhauer, A. Alam, L. Wei, Y. Chen, J. Zaumseil, A. Colsmann, R. Krupke and B. S. Flavel, *Adv. Energy Mater.*, 2016, **6**, 1600890.
22 R. Si, L. Wei, H. Wang, D. Su, S. H. Mushrif and Y. Chen, *Chem. – Asian J.*, 2014, **9**, 868–877.
23 T. Fukumaru, F. Toshimitsu, T. Fujigaya and N. Nakashima, *Nanoscale*, 2014, **6**, 5879–5886.
24 H. Zhao, L. H. Guo and Y. F. Lian, *RSC Adv.*, 2020, **10**, 21643–21649.
25 G. S. Tulevski, A. D. Franklin, D. Frank, J. M. Lobez, Q. Cao, H. Park, A. Afzali, S. J. Han, J. B. Hannon and W. Haensch, *ACS Nano*, 2014, **8**, 8730–8745.
26 L. J. Liu, J. Han, L. Xu, J. S. Zhou, C. Y. Zhao, S. J. Ding, H. W. Shi, M. M. Xiao, L. Ding, Z. Ma, C. H. Jin, Z. Y. Zhang and L. M. Peng, *Science*, 2020, **368**, 850–856.
27 M. Tange, T. Okazaki and S. Iijima, *ACS Appl. Mat. Interfaces*, 2012, **4**, 6458–6462.
28 E. Gaufres, N. Y. W. Tang, F. Lapointe, J. Cabana, M. A. Nadon, N. Cottenye, F. Raymond, T. Szkopek and R. Martel, *Nat. Photonics*, 2014, **8**, 73–79.
29 A. I. Chernov, P. V. Fedotov, H. E. Lim, Y. Miyata, Z. Liu, K. Sato, K. Suenaga, H. Shinohara and E. D. Obraztsova, *Nanoscale*, 2018, **10**, 2936–2943.
30 S. van Bezouw, D. H. Arias, R. Ihly, S. Cambre, A. J. Ferguson, J. Campo, J. C. Johnson, J. Defillet, W. Wenseleers and J. L. Blackburn, *ACS Nano*, 2018, **12**, 6881–6894.
31 F. Yang, M. Wang, D. Q. Zhang, J. Yang, M. Zheng and Y. Li, *Chem. Rev.*, 2020, **120**, 2693–2758.
32 H. Gui, J. K. Streit, J. A. Fagan, A. R. H. Walker, C. W. Zhou and M. Zheng, *Nano Lett.*, 2015, **15**, 1642–1646.
33 A. Graf, Y. Zakharko, S. P. Schiessl, C. Backes, M. Pfohl, B. S. Flavel and J. Zaumseil, *Carbon*, 2016, **105**, 593–599.
34 G. S. Tulevski, A. D. Franklin and A. Afzali, *ACS Nano*, 2013, **7**, 2971–2976.
35 L. Wei, B. S. Flavel, W. S. Li, R. Krupke and Y. Chen, *Nanoscale*, 2017, **9**, 11640–11646.
36 J. W. T. Seo, N. L. Yoder, T. A. Shastry, J. J. Humes, J. E. Johns, A. A. Green and M. C. Hersam, *J. Phys. Chem. Lett.*, 2013, **4**, 2805–2810.
37 H. W. Lee, Y. Yoon, S. Park, J. H. Oh, S. Hong, L. S. Liyanage, H. Wang, S. Morishita, N. Patil, Y. J. Park, J. J. Park, A. Spakowitz, G. Galli, F. Gygi, P. H. S. Wong, J. B. H. Tok, J. M. Kim and Z. Bao, *Nat. Commun.*, 2011, **2**, 541.
38 A. Nish, J. Y. Hwang, J. Doig and R. J. Nicholas, *Nat. Nanotechnol.*, 2007, **2**, 640–646.
39 M. S. Arnold, A. A. Green, J. F. Hulvat, S. I. Stupp and M. C. Hersam, *Nat. Nanotechnol.*, 2006, **1**, 60–65.
40 K. S. Mistry, B. A. Larsen and J. L. Blackburn, *ACS Nano*, 2013, **7**, 2231–2239.
41 F. A. Lemasson, T. Strunk, P. Gerstel, F. Hennrich, S. Lebedkin, C. Barner-Kowollik, W. Wenzel, M. M. Kappes and M. Mayor, *J. Am. Chem. Soc.*, 2011, **133**, 652–655.
42 P. Zhang, W. H. Yi, L. Bai, Y. L. Tian, J. Hou, W. Q. Jin, J. H. Si and X. Hou, *Chem. – Asian J.*, 2019, **14**, 3855–3862.
43 X. Wei and X. Maimaitiyiming, *RSC Adv.*, 2019, **9**, 32753–32758.
44 M. Tange, T. Okazaki and S. Iijima, *J. Am. Chem. Soc.*, 2011, **133**, 11908–11911.
45 G. J. Brady, Y. Joo, S. S. Roy, P. Gopalan and M. S. Arnold, *Appl. Phys. Lett.*, 2014, **104**, 083107.
46 J. S. Tang, Q. Cao, G. Tulevski, K. A. Jenkins, L. Nela, D. B. Farmer and S. J. Han, *Nat. Electron.*, 2018, **1**, 191–196.
47 W. Gomulya, G. Diaz Costanzo, E. J. Figueiredo de Carvalho, S. Z. Bisri, V. Derenskyi, M. Fritsch, N. Froehlich, S. Allard, P. Gordiichuk, A. Herrmann, S. J. Marrink, M. C. dos Santos, U. Scherf and M. A. Loi, *Adv. Mater.*, 2013, **25**, 2948–2956.
48 J. Gu, J. Han, D. Liu, X. Yu, L. Kang, S. Qiu, H. Jin, H. Li, Q. Li and J. Zhang, *Small*, 2016, **12**, 4993–4999.
49 A. Chortos, I. Pochorovski, P. Lin, G. Pitner, X. Z. Yan, T. Z. Gao, J. W. F. To, T. Lei, J. W. Will, H. S. P. Wong and Z. N. Bao, *ACS Nano*, 2017, **11**, 5660–5669.
50 H. Wang, G. I. Koleilat, P. Liu, G. Jimenez-Oses, Y.-C. Lai, M. Vosgueritchian, Y. Fang, S. Park, K. N. Houk and Z. Bao, *ACS Nano*, 2014, **8**, 2609–2617.
51 C. Wang, L. Qian, W. Xu, S. Nie, W. Gu, J. Zhang, J. Zhao, J. Lin, Z. Chen and Z. Cui, *Nanoscale*, 2013, **5**, 4156–4161.
52 X. S. Yang, T. H. Liu, R. M. Li, X. X. Yang, M. Lyu, L. Fang, L. Zhang, K. Wang, A. Q. Zhu, L. Y. Zhang, C. G. Qiu, Y. Z. Zhang, X. Wang, L. M. Peng, F. Yang and Y. Li, *J. Am. Chem. Soc.*, 2021, **143**, 10120–10130.
53 T. Z. Gao, Z. H. Sun, X. Z. Yan, H. C. Wu, H. P. Yan and Z. N. Bao, *Small*, 2020, **16**, 2000923.
54 N. Nakashima, M. Fukuzawa, K. Nishimura, T. Fujigaya, Y. Kato and A. Staykov, *J. Am. Chem. Soc.*, 2020, **142**, 11847–11856.

55 J. Y. Hwang, A. Nish, J. Doig, S. Douven, C. W. Chen, L. C. Chen and R. J. Nicholas, *J. Am. Chem. Soc.*, 2008, **130**, 3543–3553.
56 Y. Li, M. Zheng, J. Yao, W. Gong, Y. Li, J. Tang, S. Feng, R. Han, Q. Sui, S. Qiu, L. Kang, H. Jin, D. Sun and Q. Li, *Adv. Funct. Mater.*, 2021, 2107119.
57 T. Lei, X. Chen, G. Pitner, H. S. P. Wong and Z. Bao, *J. Am. Chem. Soc.*, 2016, **138**, 802–805.
58 B. S. Flavel, K. E. Moore, M. Pfohl, M. M. Kappes and F. Hennrich, *ACS Nano*, 2014, **8**, 1817–1826.
59 X. Zeng, D. H. Yang, H. P. Liu, N. G. Zhou, Y. C. Wang, W. Y. Zhou, S. S. Xie and H. Kataura, *Adv. Mater. Interfaces*, 2018, **5**, 1700727.
60 J. M. Cui, W. Su, D. H. Yang, S. L. Li, X. J. Wei, N. G. Zhou, W. Y. Zhou, S. S. Xie, H. Kataura and H. P. Liu, *ACS Appl. Nano Mater.*, 2019, **2**, 343–350.
61 Y. Yomogida, T. Tanaka, M. Tsuzuki, X. J. Wei and H. Kataura, *ACS Appl. Nano Mater.*, 2020, **3**, 11289–11297.
62 D. H. Yang, L. H. Li, X. J. Wei, Y. C. Wang, W. Y. Zhou, H. Kataura, S. S. Xie and H. P. Liu, *Sci. Adv.*, 2021, **7**, eabe0084.
63 S. Yoo, W. H. Yi, A. Khalid, J. H. Si and X. Hou, *Chem. Lett.*, 2020, **49**, 1154–1158.
64 J. Wang, T. D. Nguyen, Q. Cao, Y. L. Wang, M. Y. C. Tan and M. B. Chan-Park, *ACS Nano*, 2016, **10**, 3222–3232.
65 R. M. Jain, M. Ben-Naim, M. P. Landry and M. S. Strano, *J. Phys. Chem. C*, 2015, **119**, 22737–22745.
66 G. W. Wang, X. J. Wei, T. Tanaka and H. Kataura, *Phys. Status Solidi B*, 2017, **254**, 1700294.
67 J. G. Clar, C. A. S. Batista, S. Youn, J. C. J. Bonzongo and K. J. Ziegler, *J. Am. Chem. Soc.*, 2013, **135**, 17758–17767.
68 S. Zanoni, B. P. Watts and K. Tvrdy, *ACS Appl. Mat. Interfaces*, 2021, **13**, 33635–33643.
69 G. W. Wang, T. Tanaka, X. J. Wei, M. Yudasaka, A. Hirano and H. Kataura, *Carbon*, 2020, **156**, 422–429.
70 M. Dolan, B. P. Watts and K. Tvrdy, *Carbon*, 2021, **171**, 597–609.
71 T. Khamidullin, S. Galyaltdinov, A. Valimukhametova, V. Brusko, A. Khannanov, S. Maat, I. Kalinina and A. M. Dimiev, *Carbon*, 2021, **178**, 157–163.
72 Y. Matsunaga, J. Hirotani, Y. Ohno and H. Omachi, *Appl. Phys. Express*, 2021, **14**, 017001.
73 C. Y. Khripin, J. A. Fagan and M. Zheng, *J. Am. Chem. Soc.*, 2013, **135**, 6822–6825.
74 M. Lyu, B. Meany, J. Yang, Y. Li and M. Zheng, *J. Am. Chem. Soc.*, 2019, **141**, 20177–20186.
75 J. A. Fagan, E. H. Haroz, R. Ihly, H. Gui, J. L. Blackburn, J. R. Simpson, S. Lam, A. R. H. Walker, S. K. Doorn and M. Zheng, *ACS Nano*, 2015, **9**, 5377–5390.
76 H. Li, G. Gordeey, O. Garrity, S. Reich and B. S. Flavel, *ACS Nano*, 2019, **13**, 2567–2578.
77 S. Cambre and W. Wenseleers, *Angew. Chem., Int. Ed.*, 2011, **50**, 2764–2768.
78 T. P. Tyler, T. A. Shastry, B. J. Leever and M. C. Hersam, *Adv. Mater.*, 2012, **24**, 4765–4768.
79 L. Scharfenberg and M. Mertig, *Phys. Status Solidi A*, 2015, **212**, 1395–1398.
80 M. Jang, S. Kim, H. Jeong and S. Y. Ju, *Nanotechnology*, 2016, **27**, 41LT01.
81 D. L. Zhong, Z. Y. Zhang, L. Ding, J. Han, M. M. Xiao, J. Si, L. Xu, C. G. Qiu and L. M. Peng, *Nat. Electron.*, 2018, **1**, 40–45.
82 L. J. Liu, L. Ding, D. L. Zhong, J. Han, S. Wang, Q. H. Meng, C. G. Qiu, X. Y. Zhang, L. M. Peng and Z. Y. Zhang, *ACS Nano*, 2019, **13**, 2526–2535.
83 H. W. Shi, L. Ding, D. L. Zhong, J. Han, L. J. Liu, L. Xu, P. K. Sun, H. Wang, J. S. Zhou, L. Fang, Z. Y. Zhang and L. M. Peng, *Nat. Electron.*, 2021, **4**, 405–415.
84 Y. O. Xie, D. L. Zhong, C. W. Fan, X. S. Deng, L. M. Peng and Z. Y. Zhang, *Adv. Electron. Mater.*, 2021, **7**, 2100202.
85 H. Zhang, L. Xiang, Y. J. Yang, M. M. Xiao, J. Han, L. Ding, Z. Y. Zhang, Y. F. Hu and L. M. Peng, *ACS Nano*, 2018, **12**, 2773–2779.
86 S. Qiu, K. Wu, B. Gao, L. Li, H. Jin and Q. Li, *Adv. Mater.*, 2019, **31**, 1800750.
87 A. Corletto and J. G. Shapter, *Adv. Sci.*, 2021, **8**, 2001778.
88 B. Gao, X. P. Zhang, S. Qiu, H. H. Jin, Q. J. Song and Q. W. Li, *Carbon*, 2019, **146**, 172–180.
89 B. A. MacLeod, N. J. Stanton, I. E. Gould, D. Wesenberg, R. Ihly, Z. R. Owczarczyk, K. E. Hurst, C. S. Fewox, C. N. Folmar, K. H. Hughes, B. L. Zink, J. L. Blackburn and A. J. Ferguson, *Energy Environ. Sci.*, 2017, **10**, 2168–2179.
90 M. D. Bishop, G. Hills, T. Srimani, C. Lau, D. Murphy, S. Fuller, J. Humes, A. Ratkovich, M. Nelson and M. M. Shulaker, *Nat. Electron.*, 2020, **3**, 492–501.
91 X. He, H. Htoon, S. K. Doorn, W. H. P. Pernice, F. Pyatkov, R. Krupke, A. Jeantet, Y. Chassagneux and C. Voisin, *Nat. Mater.*, 2018, **17**, 663–670.
92 Z. Ma, L. J. Yang, L. J. Liu, S. Wang and L. M. Peng, *ACS Nano*, 2020, **14**, 7191–7199.
93 D. D. Tune and B. S. Flavel, *Adv. Energy Mater.*, 2018, **8**, 1703241.
94 W. Su, D. H. Yang, J. M. Cui, F. T. Wang, X. J. Wei, W. Y. Zhou, H. Kataura, S. S. Xie and H. P. Liu, *Carbon*, 2020, **163**, 370–378.
95 Y. Q. Liang, M. M. Xiao, D. Wu, Y. X. Lin, L. J. Liu, J. P. He, G. J. Zhang, L. M. Peng and Z. Y. Zhang, *ACS Nano*, 2020, **14**, 8866–8874.
96 G. Ao, J. K. Streit, J. A. Fagan and M. Zheng, *J. Am. Chem. Soc.*, 2016, **138**, 16677–16685.
97 Y. Yang, A. Sharma, G. Noetinger, M. Zheng and A. Jagota, *J. Phys. Chem. C*, 2020, **124**, 9045–9055.